

Efficient upconverted photocurrent through an Auger process in disklike InAs quantum structures for intermediate-band solar cells

David M. Tex,^{1,2} Itaru Kamiya,³ and Yoshihiko Kanemitsu^{1,2,*}¹*Institute for Chemical Research, Kyoto University, Uji, Kyoto 611-0011, Japan*²*JST, CREST, Uji, Kyoto 611-0011, Japan*³*Toyota Technological Institute, Nagoya, Aichi 468-8511, Japan*

(Received 26 October 2012; revised manuscript received 24 May 2013; published 10 June 2013)

The mechanisms of upconverted photocurrent in InAs quantum structures embedded in $\text{Al}_x\text{Ga}_{1-x}\text{As}$ were studied with simultaneous measurements of photoluminescence and photocurrent spectra. Efficient upconversion was verified in samples with and without quantum dots. The dominant upconversion process from low temperatures to room temperature was found to occur through an Auger process in disklike InAs quantum structures. The results suggest the importance of shallow energy levels, which enable upconversion and efficient carrier extraction through multiparticle interactions. The disklike structure was concluded to be a suitable intermediate-band structure in terms of the energy conversion efficiency.

DOI: [10.1103/PhysRevB.87.245305](https://doi.org/10.1103/PhysRevB.87.245305)

PACS number(s): 84.60.Jt, 72.40.+w, 73.50.Pz, 78.66.Fd

I. INTRODUCTION

Semiconductor crystals in bulk form have been widely used in photovoltaic technologies. The single-junction solar cell (SC) conversion efficiency is intrinsically limited to 31% by the material's band-gap energy.¹ This inherits two types of losses: transmission of photons that have lower energy than the band gap, and thermalization of the excess energy of photons with higher energy than the band gap due to relaxation. Instead of relying on multijunction SCs, which adapt the bulk structure to the solar spectrum,² both losses can also be significantly reduced by adjusting the carrier dynamics with quantum structures. This enables us to design material properties as required, and thereby, a better understanding of multiparticle interactions in quantum structures provide a detailed insight into the energy conversion processes for SCs.

The transmission losses in SCs can be substantially reduced by the design of intermediate states forming intermediate bands (IB),³ wherein upconversion generates highly excited electrons and holes through energy transfer between subband-gap-energy particles. On the other hand, relaxation losses are reduced by carrier multiplication (CM),^{4,5} in which highly excited electrons relax through the formation of two or more electron-hole (e-h) pairs. In both IBs and CMs, multiparticle interactions play a crucial role,⁶ and this requires suited quantum structures such as quantum dots (QDs) and quantum wells (QWs). However, the design principle of quantum structures for achieving considerable high efficiencies of IB and CM SCs is unknown. Therefore, it is imperative to investigate which quantum structure can achieve high efficiencies. In particular, InAs-based IBs have attracted much attention because the small band gap allows them to absorb infrared (IR) photons and high crystal quality can be achieved for a wide range of growth conditions on GaAs (which is the material closest to the ideal band gap of the single-junction SC). Due to a lattice mismatch of about 7% between InAs and GaAs or AlGaAs, different InAs quantum structures are formed in epitaxial growth.^{7,8} After the formation of the two-dimensional (2D) wetting layer (WL), which is one monolayer (ML) in height, 2D disklike structures with heights of two and three MLs are formed upon the addition of InAs.⁹ We believe that the electronic structure

of the latter plays an important role in upconversion and refer to these structures as quantum well islands (QWIs). As growth proceeds, strain relaxation occurs partly through the formation of quantum dots (QDs) for InAs deposition equivalent to about 1.7 ML.⁹ Each quantum structure forms a set of confined electron and hole states, which, in principle, may contribute to the generation of photocarriers under IR illumination.¹⁰

Meanwhile, the majority of works investigating IB SCs have focused on dense QD arrays that form a nearly perfect IB,¹¹ because an ideal interaction between delocalized electronic states results in an efficiency of 46% for unconcentrated solar light.¹² However, the band formation is not essential for the IB SC concept.¹³ An intermediate state which provides a localized electronic state is sufficient. Besides thermal excitation, two local upconversion mechanisms must be considered: (i) a carrier generated by the first photon in the localized state absorbing a second photon [local two-step two-photon absorption (TS-TPA)],^{3,14} and (ii) upconversion of a carrier via an Auger process.^{15,16} The latter is a multiparticle interaction between excited carriers and enables a variety of upconversion processes. Upconverted photoluminescence (UPL) from InAs quantum structures at low temperatures has been investigated,^{17,18} and the QWI was suggested as the quantum structure responsible for the upconversion.¹⁹ However, the mechanisms responsible for efficient upconverted photocurrent (UPC) (=photocurrent by upconversion of IR photons) has remained unclear so far: the influence of multiparticle mechanisms²⁰ has not been evaluated until now, while absorption is often considered to be essential.

In this work, we investigate the upconversion mechanisms in InAs quantum structures. Our novel sample structure enables the study of intrinsic upconversion properties of the QWIs. With the first simultaneous observation of UPL excitation and UPC excitation spectra, we find that the energetically shallow QWIs (high quantized energy) may be more suitable than the deep QDs for enhancing the SC conversion efficiency. Simultaneous measurements are required to trace the spectra from low to high temperatures. Our data clearly indicate that efficient upconversion in InAs occurs through a multiparticle Auger process rather than through a TS-TPA process. Finally we discuss the impact of our results on IB SCs.

This paper is organized as follows. In Sec. II we present our novel sample structures and a fundamental UPC excitation spectrum. Section III discusses the UPL excitation spectra of InAs layers with and without QDs. In Sec. IV the origin and upconversion mechanism of the efficient UPC generation is verified. The estimation of the efficiency limits of upconversion through multiparticle interactions in QWIs is given in the final Sec. V.

II. EXPERIMENT AND SAMPLE STRUCTURES

The sample structures shown in Fig. 1 were prepared by molecular beam epitaxy under conditions similar to those

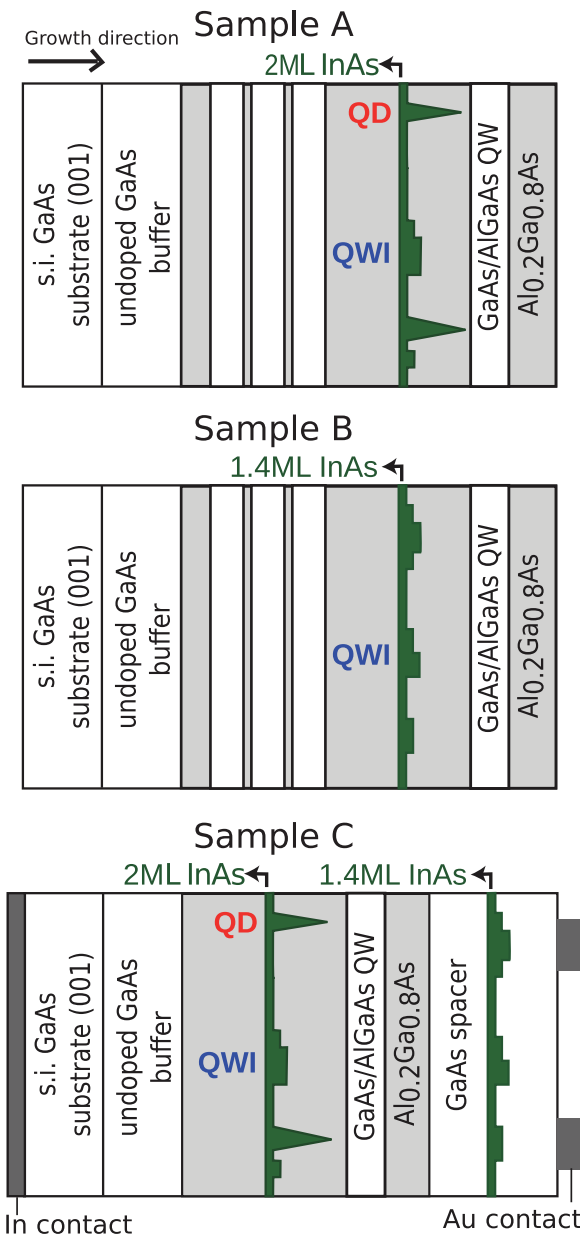


FIG. 1. (Color online) Sample structures. Sample A: The active region consists of 2 ML InAs. Sample B: The active region consists of 1.4 ML InAs in the AlGaAs matrix. Sample C: The active region consists of 2 ML InAs and the GaAs/AlGaAs QW in the AlGaAs matrix and 1.4 ML InAs in the top GaAs layer.

TABLE I. Overview of samples. For each InAs layer this table summarizes the deposited thickness, the type of surrounding barrier, the formation of QDs, and the formation of QWIs. Note that sample C contains two InAs layers. Please refer to Fig. 1 for the detailed structures.

Sample	InAs	Barrier	QD	QWI
A	2.2 ML	AlGaAs	Yes	Yes
B	1.4 ML	AlGaAs	No	Yes
C	1.4 ML	GaAs	No	Yes
	2.0 ML	AlGaAs	Yes	Yes

described in our previous publication.¹⁹ The characteristics of the samples used are summarized in Table I. For all samples a nominally undoped structure was grown on top of a semi-insulating (s.i.) GaAs (001) substrate and a GaAs buffer. In samples A and B a single InAs layer and four GaAs/AlGaAs QWs (three below and one above the InAs layer) were grown in an AlGaAs matrix. The role of the QWs is to improve the UPL signals.¹⁹ Sample A has a 2.2-ML-thick InAs layer embedded in AlGaAs. With this amount of InAs, both QWIs and QDs are formed. Sample structure B has an InAs deposition below critical thickness and therefore QWIs are formed but QDs do not exist. For sample C two different InAs layers are introduced, an AlGaAs layer containing 2 ML InAs and a GaAs/AlGaAs QW, and a top GaAs layer containing 1.4 ML InAs.

The QWI structures have smaller height and larger in-plane extension, as shown with atomic force microscopy (AFM) image in the inset of Fig. 2. The confined states are shallow, and exciton movement is weakly restricted in the in-plane direction. By using two InAs layers in one sample the influence of the barrier height is investigated. The incorporation into one sample allows accurate comparison. Electrical measurements were performed on sample C. The bottom electrical contact was formed by the In layer that remained after detaching the sample from the Mo block used for growth. The top electrode consisted of ≈ 300 nm of Au sputtered on the masked sample.

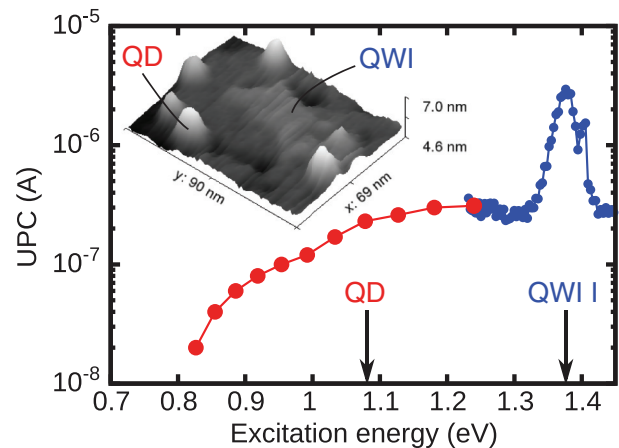


FIG. 2. (Color online) UPC excitation spectrum for sample C. The two main features are photocurrent due to excitation of the QWIs and QDs. The indicated energy levels of the shallowest QWI I and the QDs were determined from PL. Inset: 3D AFM image with QDs and a QWI on the WL of an InAs/AlGaAs layer without capping.

The UPL and UPC measurements were performed with a cw wavelength tunable Ti:sapphire laser. The sample was mounted on the cold finger of a liquid He flow cryostat with electrical contacts. The photoluminescence (PL) was analyzed with a 50-cm spectrometer and a liquid-nitrogen-cooled Si charge-coupled device camera.

The room temperature (RT) UPC excitation spectrum of sample C is shown in Fig. 2. The shoulder around 1.08 eV corresponds to UPC from the QDs. Additionally, a novel UPC peak structure can be observed for excitation energies around 1.38 eV, corresponding to upconversion in some QWIs. This is attributed to the AlGaAs barrier which suppresses GaAs photocurrent and is in contrast to the observed shoulder in InAs/GaAs structures.^{13,21–24} The use of the AlGaAs barrier allows the study of intrinsic UPC properties of quantum structures with energy slightly below the GaAs band gap. We assign different peaks to upconversion in suited QWIs. The details are discussed in Sec. IV.

III. UP CONVERTED PHOTOLUMINESCENCE FROM SAMPLES WITH AND WITHOUT QDs

The characterization of samples A and B was performed by photoexcitation at 1.49 eV, 1 W/cm². At this energy GaAs and the InAs WL buried in the AlGaAs matrix are not excited, and the PL intensities should reflect the distribution of the different InAs quantum structures. In this section only the spectral region of the QWIs is discussed. The spectral regions of GaAs and AlGaAs in similar samples are discussed in Ref. 19. The PL spectra of the QWIs in samples with and without QDs are shown in Figs. 3(a) and 3(b). In both samples, two peaks

were observed, which we assigned to the 2- and 3-ML QWI, respectively. The QD PL peak is shown in the inset of Fig. 3(a). We found that for the sample with QD formation the peak intensity of the 3-ML QWI is larger than that for the sample without QDs. This indicates a higher density of 3-ML QWIs for larger amounts of InAs deposition. The assignment of 2- and 3-ML peak energies was confirmed by comparing the peak positions with those obtained from an eight-band $\mathbf{k} \cdot \mathbf{p}$ calculation. The predicted values of 1.46 and 1.39 eV for the 2- and 3-ML QWI, respectively, are in good agreement with the experiment.¹⁹

When the QWIs are excited with low-energy photons, high-energy photons are emitted from the GaAs/AlGaAs QWs and the InAs/AlGaAs WL. This is UPL due to upconversion of electrons and holes in an InAs quantum structure and successive capture and radiative recombination in the QWs with higher quantized energy levels. The UPL excitation spectra for detection energy at the InAs/AlGaAs WL are shown in Fig. 4. The UPL peak energies due to recombination at the WL are at about 1.7 eV [(a) 1.72 eV, (b) 1.69 eV]. The excitation spectrum in Fig. 4(a) is for the sample containing QDs. It confirms strong upconversion as long as the 3-ML QWI is excited, and the intensity drops quickly for excitation energies below the 3-ML QWI energy. No UPL is observed for excitation of the QD. Since TS-TPA upconversion should occur when the QD ground state is excited, the data suggest that the TS-TPA process is not responsible for the efficient upconversion observed. The onset of the distinct decrease in the UPL intensity for lower energies is the experimentally defined critical energy. To confirm that the experimental critical energy [Fig. 4(a), green vertical broken line] in samples

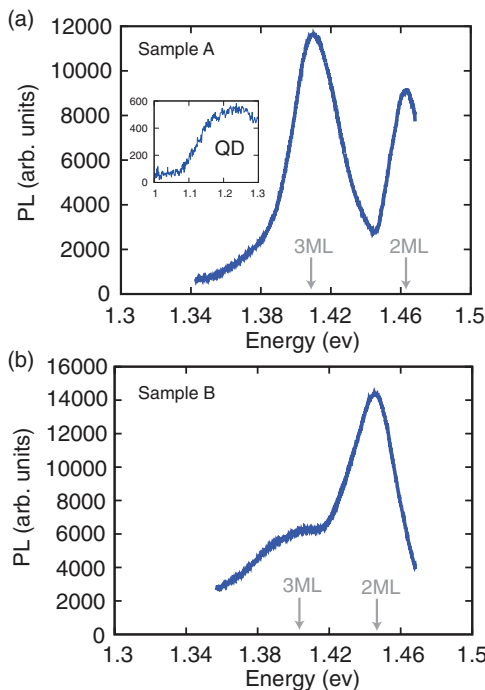


FIG. 3. (Color online) PL at about 4 K for excitation with 1.49 eV, 1 W/cm². PL of QWI region for (a) sample containing QDs and (b) sample without QDs. The peak positions of the 2- and 3-ML-thick QWIs are indicated with arrows. Inset: QD PL for sample A.

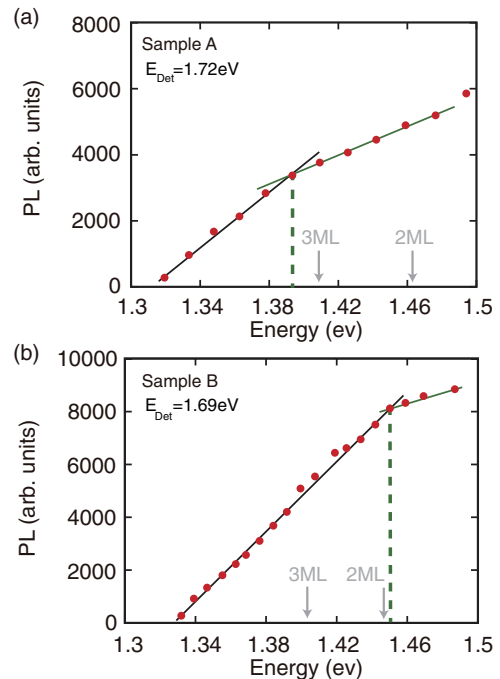


FIG. 4. (Color online) UPL excitation spectra at about 4 K for excitation with 10 W/cm². Excitation spectra for (a) sample containing QDs and (b) sample without QDs. The arrows indicate the peak positions of the 2- and 3-ML-thick QWI PL, respectively.

with QDs is not due to an excited or interface states in the QD, the same experiment was performed for the sample containing only QWIs. The result is shown in Fig. 4(b). Here, efficient upconversion is observed as long as the 2-ML QWI is excited. Three-ML QWIs do exist in this sample; however, their density is lower than that of the 2-ML QWIs. Therefore, only a small shoulder is observed for excitation of the 3-ML QWI. The overall linear trend for increasing energies is attributed to the successive contribution of the increasing number of excited QWI states close to the critical energy.

Because the excitation spectra reflect strong correlation of the QWI PL and UPL in both samples we conclude that the QWIs are responsible for efficient upconversion.

IV. UPCONVERSION MECHANISMS IN QWIs

Now we discuss the UPC in sample C. PL spectra at varied temperatures shown in Fig. 5(a) are obtained to determine the QWI energy levels. The sample contains energetically shallow and deep states, i.e., high- and low-emission energies, respectively. The InAs layer embedded in the AlGaAs mainly forms shallow 2- and 3-ML QWIs and deep QDs. The InAs layer in the GaAs forms shallow 2-ML and deep 3-ML QWIs, but no QDs, as illustrated in Fig. 1(c). The 2- and 3-ML

QWIs in the AlGaAs layer are referred to as QWIs I and II, respectively. The 2- and 3-ML QWIs in the GaAs layer are labeled QWI III and IV. The energy levels of the QWI states are determined from fits to the PL spectra. For low temperatures, the GaAs/AlGaAs QW, QWIs, and QDs can be identified (the QW peak at 1.685 eV and the QD peak at 1.17 eV are not shown here). The InAs/AlGaAs WL emission is close to that of the QW. The PL spectrum is classified into three regions: the GaAs region with energies higher than the GaAs donor-acceptor peak, the shallow QWI region, and the deep QWI and QD region. In the shallow QWI region, three peaks are identified. From high to low energies, QWIs I, III, and II are indicated in Fig. 5(b). The PL peak energies can be determined up to 100 K, but for temperatures above 100 K, the QWI peak shift is assumed to follow the trend of the GaAs band-gap redshift. Comparing of the RT energy positions inferred from Fig. 5(a) and the peak energies in Fig. 2 shows that only shallow QWIs contribute efficiently to UPC, although the QD density is severalfold compared to the QWI density, measured on uncapped samples.

The UPC excitation spectra for different temperatures are shown in Fig. 6(a). The plotted data sets are offset for clarity.

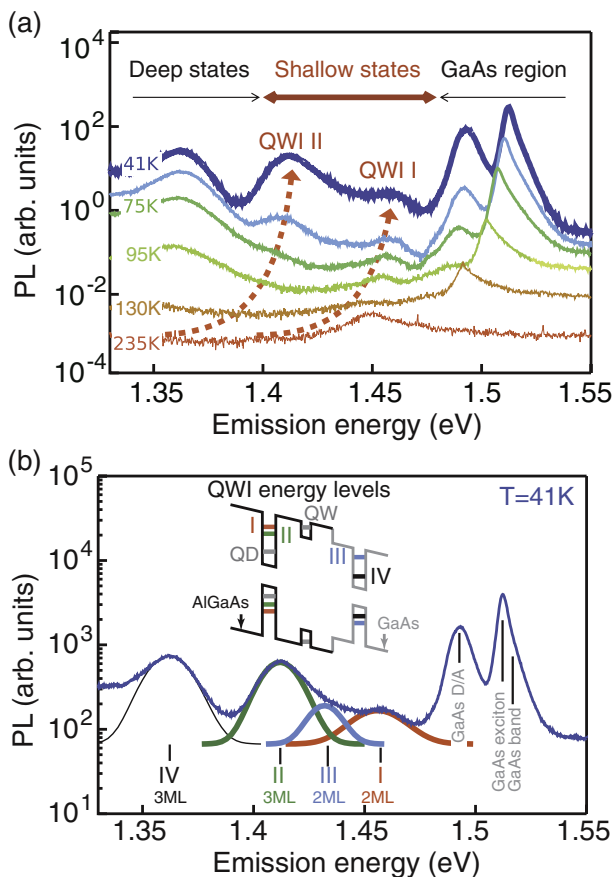


FIG. 5. (Color online) (a) PL spectra under 1.73 eV excitation (500 mW/cm^2) at varied temperatures 41–235 K. The spectra are offset for clarity. (b) Peak assignment and deconvolution of the PL spectrum at 41 K. Inset: Band diagram.

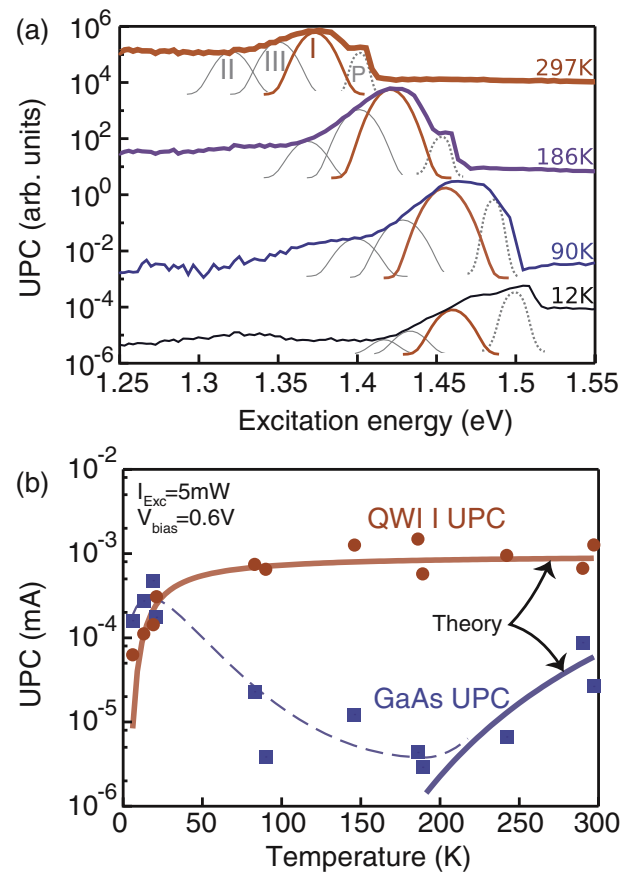


FIG. 6. (Color online) (a) UPC excitation spectra from 12 K to RT. Excitation $\approx 500 \text{ mW/cm}^2$. The spectra are offset for clarity. I, II, and III mark the peak positions of the shallow QWIs, as determined from PL. The phonon replicas (P) are shown with dotted lines. (b) The UPC temperature trend for excitation of QWI I and GaAs. The theoretical solid curves are discussed in the text.

The absolute values of the UPC for excitation of QWI I and the GaAs band gap are shown in Fig. 6(b). We emphasize that the UPC excitation spectra in Fig. 6(a) exhibit a peak for direct excitation of the shallow QWI region. Only at low temperatures the peak becomes a shoulder. This is a consequence of different upconversion mechanisms. Below 100 K, the mechanism for direct excitation is sensitive to the temperature [Fig. 6(a), peak I], whereas for indirect excitation a weak temperature dependence is observed [Fig. 6(a), P]. The peak for indirect excitation is labeled as P, found at $\approx 33 \pm 3$ meV above the strongest QWI UPC peak. This energy shift coincides with the longitudinal optical phonon energy in InAs,^{25,26} and upconversion is not observed by excitation at this energy for samples not containing InAs.¹⁹ Hence, we consider processes that can be enhanced via phonon coupling in InAs. The observed weak temperature dependence can be explained by a phonon-assisted Auger process.^{27,28}

The UPC temperature trends for excitation of QWI I and the GaAs band gap are compared in Fig. 6(b). For GaAs, the initial decrease [broken curve in Fig. 6(b) is an eye guide] is explained with upconversion from a trap state^{29,30} followed by increasing thermal excitation of free carriers [blue solid curve in Fig. 6(b): an activation energy of ≈ 170 meV]. For QWI I, the upconversion efficiency increases significantly with temperature below 100 K and then saturates. This temperature dependence cannot be explained by the direct thermal activation above the AlGaAs barrier due to the relatively deeply confined states. Moreover, the TS-TPA process is an implausible explanation because the interband photon absorption temperature dependence cannot explain the observed significant UPC increase at low temperatures,^{31,32} nor excitation spectra for samples with and without QDs.³³ Therefore, we consider the Auger process for upconversion in InAs QWIs: after formation of two e-h pairs in the QWI, one e-h pair recombines and successively transfers its energy to the other carriers.

In general, the impact ionization of carriers through the Auger process implies efficient rates for thin QWIs, because the kinetic energy of the Auger carriers can overcome the barrier. By comparison of the ionized levels and the barrier height, a critical QWI energy of about 1.36 eV was estimated for low temperatures.³⁴ This is in agreement with our data, in which only QWIs with larger energy, i.e., shallow states, show strong upconversion. The peaks from these QWIs [peaks I, II, and III; also please see Fig. 5(b)] are illustrated in Fig. 6(a). The rate of Auger processes is exponentially proportional to the temperature due to the occupation probability of states required for momentum and energy conservation.^{35,36} The observed trend agrees well with the prediction for a threshold energy of 2.4 ± 0.4 meV [red solid curve in Fig. 6(b)]. Here, we attribute the initial high efficiency and low threshold energy to the unique electronic structure of the QWI. The bound to continuum ionization rates are enhanced by the spatial overlap of e-h pairs and are strongly peaked around resonances.^{35,37} These rates can be further enhanced by the confinement induced state mixing (a wave function spread in k space, which leads to relaxation of the conventional k -conservation rule).³⁸⁻⁴⁰ The above mechanisms can explain the small Auger threshold energies in the QWIs.

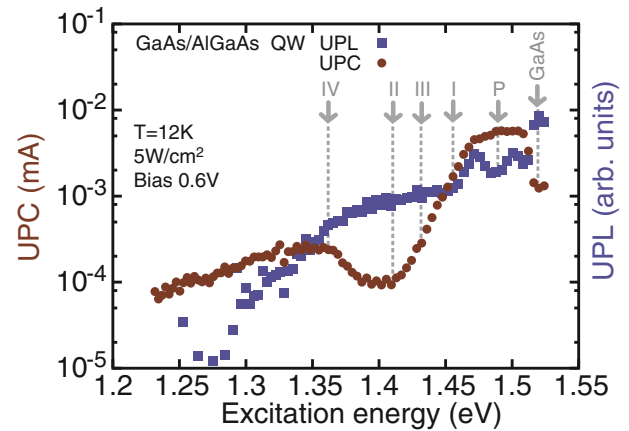


FIG. 7. (Color online) Comparison of UPL and UPC. P indicates the phonon-assisted upconversion peak. I, II, and III mark the peak positions of the shallow QWIs.

To verify that the structure of the UPC spectrum for direct excitation at low temperatures corresponds to the QWIs [Fig. 6(a)], we compare UPC and UPL excitation spectra in Fig. 7. Because the UPL signal is weak under low-density excitation, data for high-density excitation 5 W/cm^2 are presented.

The UPL intensity measured was that of radiative recombination from the GaAs/AlGaAs QW at 1.685 eV. Under small electric fields in the sample, upconverted carriers can be initially ejected to both directions (along the growth direction in Fig. 2). Therefore, UPL peaks correspond mainly to upconversion in one QWI layer. Both the UPC and the UPL excitation spectra show an overall decrease of the upconversion signal with decreasing excitation energy. This is because upconversion through the Auger process is inhibited for deeply confined states. Moreover, the abrupt changes in the excitation spectra (Fig. 7, gray arrows) correspond to the shallow QWI states. We note an opposite trend of UPC and UPL (Fig. 7, B and P). This indicates that, while the sum of UPL and UPC is proportional to the upconversion efficiency, there is a competition between recombination (UPL) and current flow (UPC). Similar but small features are observed at the peak positions of QWIs I and III. In addition, the small UPC peak at 1.35 eV is due to thermal activated upconversion from deep states. No significant signals in the UPC spectrum are detected from the deep states at low temperatures, although thermal activation increases their contribution at elevated temperatures. We also point out that UPL is observed from shallow QWIs in both InAs layers, i.e., with and without QDs. This indicates that the QWIs are responsible for the efficient upconversion.

The power dependence of UPL and UPC for excitation of QWI I is shown in Fig. 8. The measurement was performed at 20 K, allowing good comparison of UPL and UPC signals. The UPC and UPL power dependencies are shown with the red and blue data points, respectively. Both UPL and UPC signals follow a nonlinear trend close to the quadratic power dependence shown with the broken line. Because both UPL and UPC signals are due to upconversion in shallow QWIs, this indicates that a nonlinear process in the QWI is responsible for efficient upconversion.

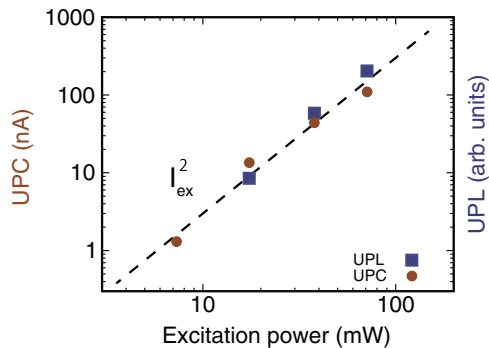


FIG. 8. (Color online) Power dependence of UPL and UPC for excitation of QWI I at 20 K. Both UPL and UPC trends indicate that a nonlinear process is responsible for the efficient upconversion in shallow QWIs. For a guide to the eye we plotted the broken line I_{ex}^2 , representing a quadratic power dependence on the excitation intensity.

We conclude that the Auger interaction between two e-h pairs formed in the QWI is the dominant upconversion process. While further investigations are required to clarify the details of the Auger ionization process, the present results suggest that multiparticle upconversion processes in QWIs are efficient due to involvement of shallow confined states. Therefore, carriers can be easily ejected from the QWI after Auger ionization. Since in QDs, efficient Auger upconversion is inhibited by the deeply confined states, TS-TPA and thermal excitation becomes important, but remain minor compared to Auger in QWIs.

V. APPLICATION TO INTERMEDIATE BANDS

In the following, we estimate the impact of the highly efficient multiparticle Auger interactions in InAs quantum structures. For the AM1.5G solar spectrum, in our InAs/Al_{0.2}Ga_{0.8}As quantum structure, the ideal additional UPC through the QWI is only 1.73 times less than that for the QD. This is determined by the fraction of photogenerated carriers en_{ph} by absorption of the spectral region between the confined state and the barrier,

$$en_{ph} = \frac{1}{2} \int_{E_{cs}}^{E_b} \phi_{sun}(E) dE, \quad (1)$$

where ϕ_{sun} is the spectral photon density, and E_b and E_{cs} the energy of the barrier and confined state, respectively. The factor $\frac{1}{2}$ implies that for every generated upconverted e-h pair two photons are required. This calculation assumes absorption edges for QWIs, QDs, and AlGaAs as given below. Because the UPC efficiency of the QWIs observed here and in previous works is approximately an order of magnitude larger than that for QDs,^{13,24} the upconversion through QWIs may result in a conversion efficiency approximately fivefold higher than that through QDs. Although the spectral absorption width of the QWI is rather narrow, the high efficiency indicates the potential for a considerable improvement of the energy conversion.

By applying a detailed balance calculation to our QWI structure, we would like to present a figure of merit for its possible application. The SC efficiency at 300 K is determined

with absorption edge for the QWI $E_{QWI} = 1.31$ eV, for the QD $E_{QD} = 1.08$ eV, and for bulk AlGaAs $E_{Al_{0.2}Ga_{0.8}As} = 1.67$ eV. We assume a refractive index of $n = 3.5$ and that for Auger upconversion half of the available photons between bulk and the quantum structure absorption edge can be converted to e-h pairs. For the detailed balance calculation we use the following method.² The open circuit voltage of a single junction is given by

$$eV_{oc} = E_g - k_B T \ln \frac{A}{en_{ph}}, \quad (2)$$

where k_B is the Boltzmann constant, T is the temperature of the solar cell, and A determines the radiative current.² The solar cell current is then approximated with

$$J = en_{ph} - Ae^{\frac{eV - E_g}{k_B T}}. \quad (3)$$

By optimizing the power, the voltage eV_m and the current J_m at the maximum power are found:

$$eV_m = eV_{oc} - k_B T \ln \left(1 + \frac{eV_m}{k_B T} \right), \quad (4)$$

and

$$J_m = \frac{en_{ph}}{1 + \frac{k_B T}{eV_m}}. \quad (5)$$

By performing this exercise we find that the AlGaAs single-junction SC including ideal QWIs can reach 35.7% conversion efficiency (AlGaAs bulk, 28.2%). Optimized real QWIs may realize conversion efficiencies higher than those of GaAs single-junction SCs by a few percent. In order to realize a total conversion efficiency increase on the order of a few percent, the QWI structures must be methodically optimized for upconversion.

VI. CONCLUSION

We performed optical and electrical measurements of InAs quantum structures. Efficient UPL was obtained through excitation of QWIs in samples with and without QDs. Using UPC excitation spectroscopy, a distinct peak structure in the energy region of the QWI has been presented. The temperature dependence of the UPC excitation spectra revealed a very small activation energy for this UPC peak, which is attributed to efficient upconversion in the QWI. Supported by complimentary UPL and UPC excitation spectra and power dependence we assigned the upconversion mechanisms in QWIs. The data revealed that the multiparticle Auger carrier dynamics are significant for UPC through upconversion in InAs quantum structures whose energy levels are shallow enough. We believe that the present work opens possibilities for development of a new field involving IB SCs based on upconversion via strong Auger interaction.

ACKNOWLEDGMENTS

The authors would like to thank T. Ihara for the help during the experiments. Part of this work was supported by JST-CREST and the Strategic Research Infrastructure Project of MEXT.

*kanemitsu@scl.kyoto-u.ac.jp

- ¹W. Shockley and H. J. Queisser, *J. Appl. Phys.* **32**, 510 (1961).
- ²C. H. Henry, *J. Appl. Phys.* **51**, 4494 (1980).
- ³A. Luque and A. Martí, *Phys. Rev. Lett.* **78**, 5014 (1997).
- ⁴J. H. Werner, S. Kolodinski, and H. J. Queisser, *Phys. Rev. Lett.* **72**, 3851 (1994).
- ⁵A. J. Nozik, *Physica E* **14**, 115 (2002).
- ⁶Y. Kanemitsu, *Acc. Chem. Res.* (2013), doi: 10.1021/ar300269z.
- ⁷D. Leonard, M. Krishnamurthy, C. M. Reaves, S. P. Denbaars, and P. M. Petroff, *Appl. Phys. Lett.* **63**, 3203 (1993).
- ⁸V. Bressler-Hill, A. Lorke, S. Varma, P. M. Petroff, K. Pond, and W. H. Weinberg, *Phys. Rev. B* **50**, 8479 (1994).
- ⁹R. Heitz, T. R. Ramachandran, A. Kalburge, Q. Xie, I. Mukhametzhanov, P. Chen, and A. Madhukar, *Phys. Rev. Lett.* **78**, 4071 (1997).
- ¹⁰The QWI or QD ground state can be considered as an intermediate state, which is a slight variation from the usually picture of the IB concept.
- ¹¹A. Luque, A. Martí, and C. Stanley, *Nat. Photonics* **6**, 146 (2012), and references therein.
- ¹²A. Luque and A. Martí, *Prog. Photovoltaics* **9**, 73 (2001).
- ¹³D. Guimard, R. Morihara, D. Bordel, K. Tanabe, Y. Wakayama, M. Nishioka, and Y. Arakawa, *Appl. Phys. Lett.* **96**, 203507 (2010).
- ¹⁴R. Hellmann, A. Euteneuer, S. G. Hense, J. Feldmann, P. Thomas, E. O. Göbel, D. R. Yakovlev, A. Waag, and G. Landwehr, *Phys. Rev. B* **51**, 18053 (1995).
- ¹⁵W. Seidel, A. Titkov, J. P. André, P. Voisin, and M. Voos, *Phys. Rev. Lett.* **73**, 2356 (1994).
- ¹⁶A. Luque, A. Martí, and Lucas Cuadra, *IEEE Trans. Electron Devices* **50**, 447 (2003).
- ¹⁷C. Kammerer, G. Cassabois, C. Voisin, C. Delalande, Ph. Roussignol, and J. M. Gérard, *Phys. Rev. Lett.* **87**, 207401 (2001).
- ¹⁸P. P. Paskov, P. O. Holtz, B. Monemar, J. M. Garcia, W. V. Schoenfeld, and P. M. Petroff, *Appl. Phys. Lett.* **77**, 812 (2000).
- ¹⁹D. M. Tex and I. Kamiya, *Phys. Rev. B* **83**, 081309(R) (2011).
- ²⁰R. Feirreira and G. Bastard, *Appl. Phys. Lett.* **74**, 2818 (1999).
- ²¹R. Oshima, A. Takata, and Y. Okada, *Appl. Phys. Lett.* **93**, 083111 (2008).
- ²²Y. Okada, T. Morioka, K. Yosida, R. Oshima, Y. Shoji, T. Inoue, and T. Kita, *J. Appl. Phys.* **109**, 024301 (2011).
- ²³A. Martí, E. Antolín, C. R. Stanley, C. D. Farmer, N. López, P. Díaz, E. Canovas, P. G. Linares, and A. Luque, *Phys. Rev. Lett.* **97**, 247701 (2006).
- ²⁴A. Luque, A. Martí, N. López, E. Antolín, E. Cánovas, C. Stanley, C. Farmer, L. J. Caballero, L. Cuadra, and J. L. Balenzategui, *Appl. Phys. Lett.* **87**, 083505 (2005).
- ²⁵P. D. Wang, N. N. Ledentsov, C. M. Sotomayor Torres, I. N. Yassievich, A. Pakhomov, A. Yu. Egorov, P. S. Kopev, and V. M. Ustinov, *Phys. Rev. B* **50**, 1604 (1994).
- ²⁶R. Heitz, M. Grundmann, N. N. Ledentsov, L. Eckey, M. Veit, D. Bimberg, V. M. Ustinov, A. Yu. Egorov, A. E. Zhukov, P. S. Kopev, and Zh. I. Alferov, *Appl. Phys. Lett.* **68**, 361 (1996).
- ²⁷N. K. Dutta and R. J. Nelson, *J. Appl. Phys.* **53**, 74 (1982).
- ²⁸Y. Yamada, H. Yasuda, T. Tayagaki, and Y. Kanemitsu, *Phys. Rev. Lett.* **102**, 247401 (2009).
- ²⁹Y. Nomura, K. Shinozaki, and M. Ishii, *J. Appl. Phys.* **58**, 1864 (1985).
- ³⁰D. M. Tex and I. Kamiya, *J. Vac. Sci. Technol., B* **30**, 02B120 (2012).
- ³¹M. O. Manasreh, F. Szmulowicz, D. W. Fischer, K. R. Evans, and C. E. Stutz, *Appl. Phys. Lett.* **57**, 1790 (1990).
- ³²F. Bras, P. Boucaud, S. Sauvage, G. Fishman, and J.-M. Gérard, *Appl. Phys. Lett.* **80**, 4620 (2002).
- ³³The weak influence of QD states on the upconversion spectra can be readily confirmed for a set of samples containing separate layers of QWIs and QDs. See Sec. III for details.
- ³⁴The critical energy is referred to as the energy from where an Auger process just barely ejects the carriers from the quantum structure into the barrier. We assumed the following parameters for estimation of the critical QWI energy at low temperatures: InAs band gap $E_1 = 0.41$ eV, GaAs band gap $E_2 = 1.52$ eV, AlGaAs band gap $E_3 = 1.82$ eV, and valence band offsets $E_{1-2} = 0.50$ eV, $E_{1-3} = 0.61$ eV, and $E_{2-3} = 0.1$ eV. Due to momentum conservation the energy is distributed differently between electron ($m_e = 0.026m_0$) and hole ($m_h = 0.41m_0$).
- ³⁵P. T. Landsberg, *Recombination in Semiconductors* (Cambridge University Press, Cambridge, UK, 2003).
- ³⁶A. R. Beattie and P. T. Landsberg, *Proc. R. Soc. London, Ser. A* **249**, 16 (1959).
- ³⁷D. I. Chepic, Al. L. Efros, A. I. Ekimov, M. G. Ivanov, V. A. Kharchenko, I. A. Kudriavtsev, and T. V. Yazeva, *J. Lumin.* **47**, 113 (1990).
- ³⁸R. I. Taylor, R. Abram, M. G. Burt, and C. Smith, *Semicond. Sci. Technol.* **5**, 90 (1990).
- ³⁹I. Robel, R. Gresback, U. Kortshagen, R. D. Schaller, and V. I. Klimov, *Phys. Rev. Lett.* **102**, 177404 (2009).
- ⁴⁰K. Ueda, T. Tayagaki, M. Fukuda, M. Fujii, and Y. Kanemitsu, *Phys. Rev. B* **86**, 155316 (2012).